


Human Adult Fibroblast-like Synoviocytes and Articular Chondrocytes Exhibit Prominent Overlap in Their Transcriptomic Signatures

Kyle Jones,¹ Marco Angelozzi,² Umesh Gangishetti,¹ Abdul Haseeb,² Charles de Charleroy,² Véronique Lefebvre,² and Pallavi Bhattaram¹ 

Objectives. Fibroblast-like synoviocytes (FLS) and articular chondrocytes (AC) derive from a common pool of embryonic precursor cells. They are currently believed to engage in largely distinct differentiation programs to build synovium and articular cartilage and maintain healthy tissues throughout life. We tested this hypothesis by deeply characterizing and comparing their transcriptomic attributes.

Methods. We profiled the transcriptomes of freshly isolated AC, synovium, primary FLS, and dermal fibroblasts from healthy adult humans using bulk RNA sequencing assays and downloaded published single-cell RNA sequencing data from freshly isolated human FLS. We integrated all data to define cell-specific signatures and validated findings with quantitative reverse transcription PCR of human samples and RNA hybridization of mouse joint sections.

Results. We identified 212 AC and 168 FLS markers on the basis of exclusive or enriched expression in either cell and 294 AC/FLS markers on the basis of similar expression in both cells. AC markers included joint-specific and pan-cartilaginous genes. FLS and AC/FLS markers featured 37 and 55 joint-specific genes, respectively, and 131 and 239 pan-fibroblastic genes, respectively. These signatures included many previously unrecognized markers with potentially important joint-specific roles. AC/FLS markers overlapped in their expression patterns among all FLS and AC subpopulations, suggesting that they fulfill joint-specific properties in all, rather than in discrete, AC and FLS subpopulations.

Conclusion. This study broadens knowledge and identifies a prominent overlap of the human adult AC and FLS transcriptomic signatures. It also provides data resources to help further decipher mechanisms underlying joint homeostasis and degeneration and to improve the quality control of tissues engineered for regenerative treatments.

INTRODUCTION

Articular joints fulfill the essential functions of connecting appendicular bone ends, allowing friction-, deformation-, and pain-free movements. Their progressive degeneration is a main feature of osteoarthritis (OA), rheumatoid arthritis (RA), and other joint diseases and a major cause of chronic pain and reduced mobility in the adult and elderly populations. These diseases are altogether highly prevalent, but no cures exist yet, and therapies have limitations. The development of better treatments is hindered by an

incomplete grasp of the phenotypic features of the main resident joint cells, even though these features are likely critical determinants of joint homeostasis and disease.

Articular cartilage and the synovium are the main inner tissues of articular joints. Articular cartilage is a structurally strong, highly resilient aneural and avascular mantle protecting bone ends. Its abundant and highly specific extracellular matrix is produced by articular chondrocytes (AC), its sole resident cells. Unlike growth plate chondrocytes (GPC), which are temporary cells undergoing proliferation, differentiation,

Dr. Lefebvre's work was supported by an Arthritis Foundation Delivering on Discovery grant and a Rheumatology Research Foundation Disease Targeted Research grant. Drs. Lefebvre and Bhattaram's work was supported by grants from the NIH National Institute of Arthritis and Musculoskeletal and Skin (R01-AR-072649 and R01-AR-070736, respectively). Dr. Bhattaram's work was supported by startup funds from the Department of Orthopaedics, Emory University.

¹Kyle Jones, BS, Umesh Gangishetti, PhD, Pallavi Bhattaram, PhD: Emory University School of Medicine, Atlanta, Georgia; ²Marco Angelozzi, PhD, Abdul Haseeb, PhD, Charles de Charleroy, MS, Véronique Lefebvre, PhD: Children's Hospital of Philadelphia, Philadelphia, Pennsylvania.

Drs. Jones and Angelozzi contributed equally to this work.

No potential conflicts of interest relevant to this article were reported.

Address correspondence Véronique Lefebvre, PhD, Children's Hospital of Philadelphia, Department of Surgery, Division of Orthopaedic Surgery, 3615 Civic Center Boulevard, Philadelphia, PA 19104 (email: lefebrev1@chop.edu); or to Pallavi Bhattaram, PhD, Emory University, School of Medicine, Departments of Orthopaedics and Cell Biology, 100 Woodruff Circle, Atlanta, GA 30322 (email: pallavi.bhattaram@emory.edu).

Submitted for publication February 17, 2021; accepted in revised form March 3, 2021.

and terminal maturation in development only, AC are permanent cells undergoing limited phenotypic changes in adulthood (1). The synovium, in contrast, is a highly cellular, vascularized, and innervated tissue. Its fibroblast-like synoviocytes (FLS) and macrophage-like synoviocytes complement each other in generating not only the synovium tissue but also the synovial fluid, which is essential for joint lubrication and articular cartilage homeostasis (2).

During development, AC and FLS originate from a common pool of mesenchymal cells characterized by growth and differentiation factor 5 (*Gdf5*) expression (3). During joint morphogenesis, nascent AC and FLS deactivate *Gdf5* and activate differentiation markers that allow them to build distinct tissues. AC express pan-cartilaginous markers, such as collagen type 2 (*COL2A1*) and aggrecan (*ACAN*), whereas FLS express pan-fibroblastic (PanF) markers, such as collagen type I (*COL1A1*) and versican (*VCAN*). In addition, AC and FLS express articular-specific genes, and there is evidence that they share some of these markers. One of them, *PRG4*, encodes proteoglycan-4 (also called lubricin), a pivotal joint lubricant. To date, however, the AC and FLS molecular signatures and the extent of their overlap are incompletely known. We help fill this gap by fully profiling and comparing the transcriptomes of both cell types. We uncover new markers for each cell and reveal an unexpected large overlap of the specific cell attributes. By expanding knowledge and predicting essential functions for many of these markers, these findings are expected to facilitate new studies on mechanisms underlying joint health and disease and on new treatment options for rheumatic diseases.

METHODS

Sample collection. Knee and hip articular cartilage and synovium were obtained under institutional ethics committee approval from individuals undergoing arthroplasty for OA or from individuals deceased with no known joint or other disease (Supplementary Table 1).

RNA isolation. Articular cartilage from tibial plateaus and from femoral heads and condyles was shaved in its entire depth while avoiding noncartilaginous tissue. It was digested with 1 mg/ml Pronase (Roche) in Dulbecco's modified Eagle medium (DMEM) containing 5% fetal calf serum (FCS) at 37°C for 1 hour, followed by 1 mg/ml collagenase B (Roche) in DMEM containing 5% FCS at 37°C overnight. Freshly isolated articular chondrocytes (fAC) were washed with phosphate-buffered saline and immediately lysed in Trizol. Synovial tissue (ST) was grinded in Trizol promptly after harvesting (PowerGen 125 Homogenizer; Fisher Scientific). To obtain primary FLS (pFLS), 100 mg of the synovium was digested with 1 mg/ml of collagenase V (Sigma-Aldrich) in DMEM containing 10% FCS for 2 hours at 37°C. Isolated cells were cultured in monolayer in DMEM with 10% FCS, with frequent medium changes to keep only adherent cells, until passage four. Total RNA was

extracted from all samples by using the Trizol method, followed by the RNeasy Kit (Qiagen). RNA concentration and integrity was assessed by using the Bioanalyzer (Agilent). All preparations used for RNA sequencing (RNA-seq) had an RNA integrity number greater than 9.0 (Supplementary Table 1).

RNA-seq assays and data analysis. As described (4), RNA libraries were generated from 1 µg RNA by using the TruSeq Library Preparation Kit (Illumina) and sequenced on the HiSeq 2500 System (Illumina). Bulk RNA-seq data from primary dermal fibroblasts (pDF) (5) and single-cell RNA-seq data from synovial cell populations (6) were downloaded from public databases (Gene Expression Omnibus [code GSE104288] and ImmPort Shared Data [code SDY998], respectively). Strand NGS software was used to align bulk RNA-seq data with the Homo sapiens (human) genome assembly GRCh37 (hg19), to eliminate duplicate reads, to calculate RNA levels in reads per kilobase per million mapped reads (RPKM), and to perform analyses. All genes that had RNA levels greater than 3 RPKM in at least one sample type were analyzed. Pairwise differential expression analyses were used to identify differentially expressed genes. Data were further analyzed by using principal component analysis, hierarchical clustering, and heat map analysis of normalized intensity values. Gene ontology matching was performed by using Ingenuity Pathway Analysis (Qiagen). Data from single-cell RNA-seq assays were analyzed by using Seurat v3. Cells with greater than 9000 and fewer than 1000 expressed genes and greater than 60% mitochondrial transcripts were excluded. Data were normalized by using the SCTransform normalization method (7) and then used in the principal component analysis and uniform manifold approximation and projection (UMAP).

Quantitative reverse transcription PCR (qRT-PCR). qRT-PCR assays were performed on the QuantStudio 5 Real-Time PCR System (Thermo Fisher Scientific). Complementary DNA (cDNA) was synthesized from 1 µg total RNA by using qScript cDNA SuperMix (Quantabio), and real-time PCR was performed by using PerfeCTa SYBR Green SuperMix (Quantabio) and appropriate primers (Supplementary Table 2). Data were quantified by using the delta-delta Ct method.

RNA in situ hybridization. Knees of 3-month-old mice were fixed in 4% paraformaldehyde for 48 hours at 4°C, demineralized in Morse's solution (22.5% formic acid, 10 g/100 ml sodium citrate) for 48 hours at 4°C, embedded in paraffin, and sectioned sagittally at 7-µm thickness. RNA in situ hybridization was performed by using specific probes (Supplementary Table 3) and RNAscope 2.5 HD Detection Reagent Kit (Advanced Cell Diagnostics). Pictures were taken by using an AxioScan.Z1 (Zeiss) instrument and processed by using Adobe Photoshop CC 19.1.6 software. Weak RNA signals were amplified by increasing the magenta color saturation, as indicated in Figures 3-5.

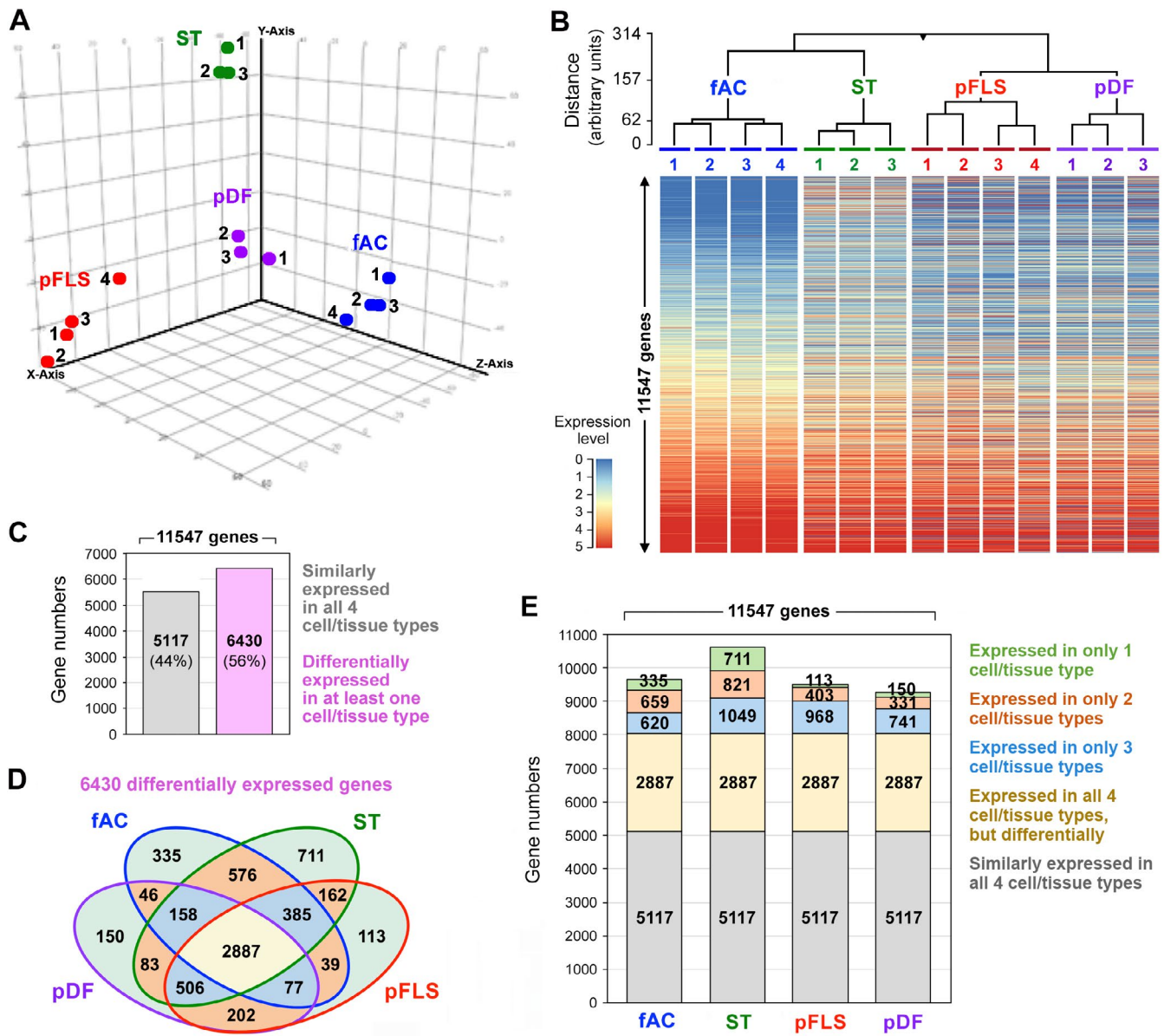


Figure 1. Global analysis of transcriptomic differences between freshly isolated articular chondrocytes (fAC), synovial tissue (ST), primary fibroblast-like synoviocytes (pFLS), and primary dermal fibroblasts (pDF). **A**, Principal component analysis showing transcriptome relationships between all samples, as assessed by bulk RNA sequencing (see Supplementary Table 4A). All 11,547 genes expressed in either or all samples were included. Principal component 1 (PC1) (x-axis), PC2 (y-axis), and PC3 (z-axis) represent 40.28%, 21.55%, and 19.82%, respectively, of the total data variation. **B**, Hierarchical clustering of three to four biological replicates for each cell/tissue type, measured in arbitrary units and combined with a heat map of gene expression. In the latter, each line represents one gene and is color coded on the basis of normalized expression level. **C**, Numbers and proportions of genes similarly and differentially expressed in the four cell/tissue types (see Supplementary Table 4A). **D**, Distribution of the 6,430 differentially expressed genes in the four cell/tissue types. Numbers indicate how many genes were detected expressed in one or several tissue/cell types, regardless of relative expression levels (see Supplementary Table 4B). **E**, Total number of genes expressed in each sample type, with indication of the numbers of genes uniquely expressed in each sample and the number of genes shared with others.

Statistics. Three or four independent samples were used per tissue/cell type. A hierarchical condition tree was generated by clustering normalized intensity values using the Euclidean similarity measure and Ward’s linkage rule. RNA-seq data were analyzed by using one-way analysis of variance and Student’s *t*-tests, and qRT-PCR data were analyzed by using Student’s *t*-test, with a *P* value less than 0.05 considered significant.

RESULTS

Evidence of a potentially major overlap of the AC and FLS transcriptomic features. To directly compare the AC and FLS transcriptomes, we performed bulk RNA-seq assays for ST; fAC; FLS-enriched primary synovial cells, or pFLS (8); and pDF (5). All samples derived from healthy-looking tissues harvested from

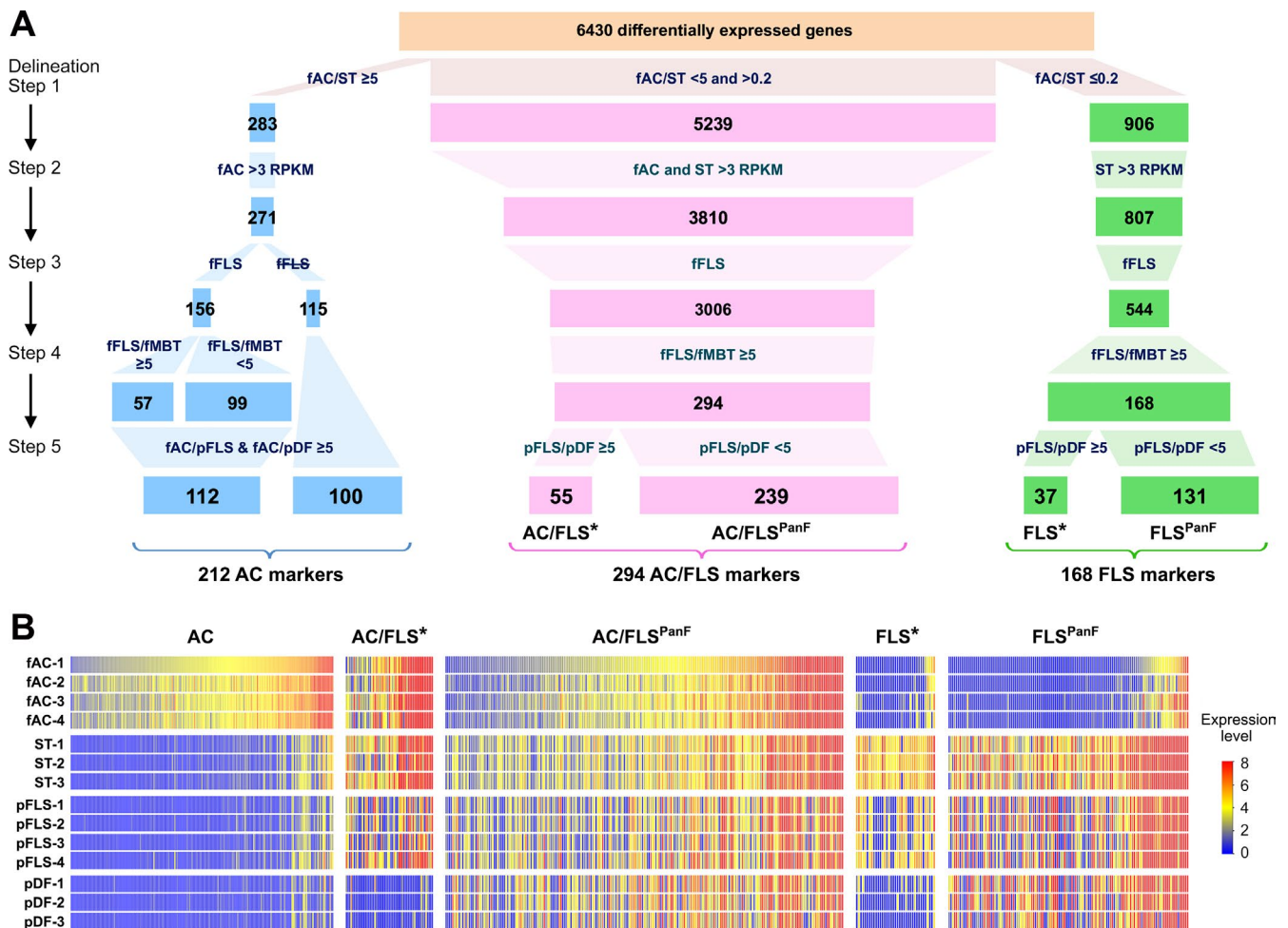


Figure 2. Delineation of lists of presumptive articular chondrocyte (AC), articular chondrocyte/fibroblast-like synoviocyte (AC/FLS), and fibroblast-like synoviocyte (FLS) marker genes. **A**, Schematic showing both the strategy used to delineate markers and the results in terms of gene numbers. See Results section and Supplementary Table 4C–F for details. **B**, Heat maps showing the relative expression of all genes constituting newly defined marker lists. Each line represents one gene and is color coded on the basis of a normalized expression level. * Joint specific. fAC, freshly isolated articular chondrocytes; fFLS, freshly isolated fibroblast-like synoviocytes; fMBT, freshly isolated macrophages, T cells and B cells; PanF, pan-fibroblastic; pDF, primary dermal fibroblasts; pFLS, primary fibroblast-like synoviocytes; RPKM, reads per kilobase per million mapped reads; ST, synovial tissue.

unrelated 19- to 66-year-old men and women with no disease deemed to substantially affect the cell/tissue transcriptomes (Supplementary Table 1).

Principal component analysis and hierarchical clustering showed that ST was transcriptionally closer to fAC than to pFLS and slightly closer to pFLS than to pDF and that pFLS and pDF still exhibited distinct features, despite some possible phenotypic drift in culture (Figure 1A and B). Together, the samples significantly expressed 11,547 genes, of which 5117 (44%) were likely house-keeping genes (less than twofold differences in expression) (Supplementary Table 4A and Figure 1C). Of the other 6430 genes, 2887 (45%) were expressed in all sample types, but differentially; 1126 (18%) were expressed in three sample types; 1108 (17%) were expressed in two sample types, with ST and fAC sharing the highest number (576); and 1309 (20%) were expressed in one sample type, with ST (711) and fAC (335) outnumbering

pFLS (113) and pDF (150) (Figure 1D and E and Supplementary Table 4B).

Beside pointing to specific transcriptomic features for each joint cell type, these data also suggested that AC and FLS share a large set of transcriptomic attributes.

Delineation of presumptive AC, AC/FLS, and FLS gene signatures.

To identify unique and shared AC and FLS markers, we undertook a five-step delineation process (Figure 2A). Because cell types are defined not only by the genes that they have the exclusivity to express but also by the genes that they express much more highly than other cell types, we first distributed the 6430 differentially expressed genes into three groups on the basis of expression level in fAC relative to ST (fAC/ST ratio; Figure 2A and Supplementary Table 4C). The first group comprised 283 genes exclusively or

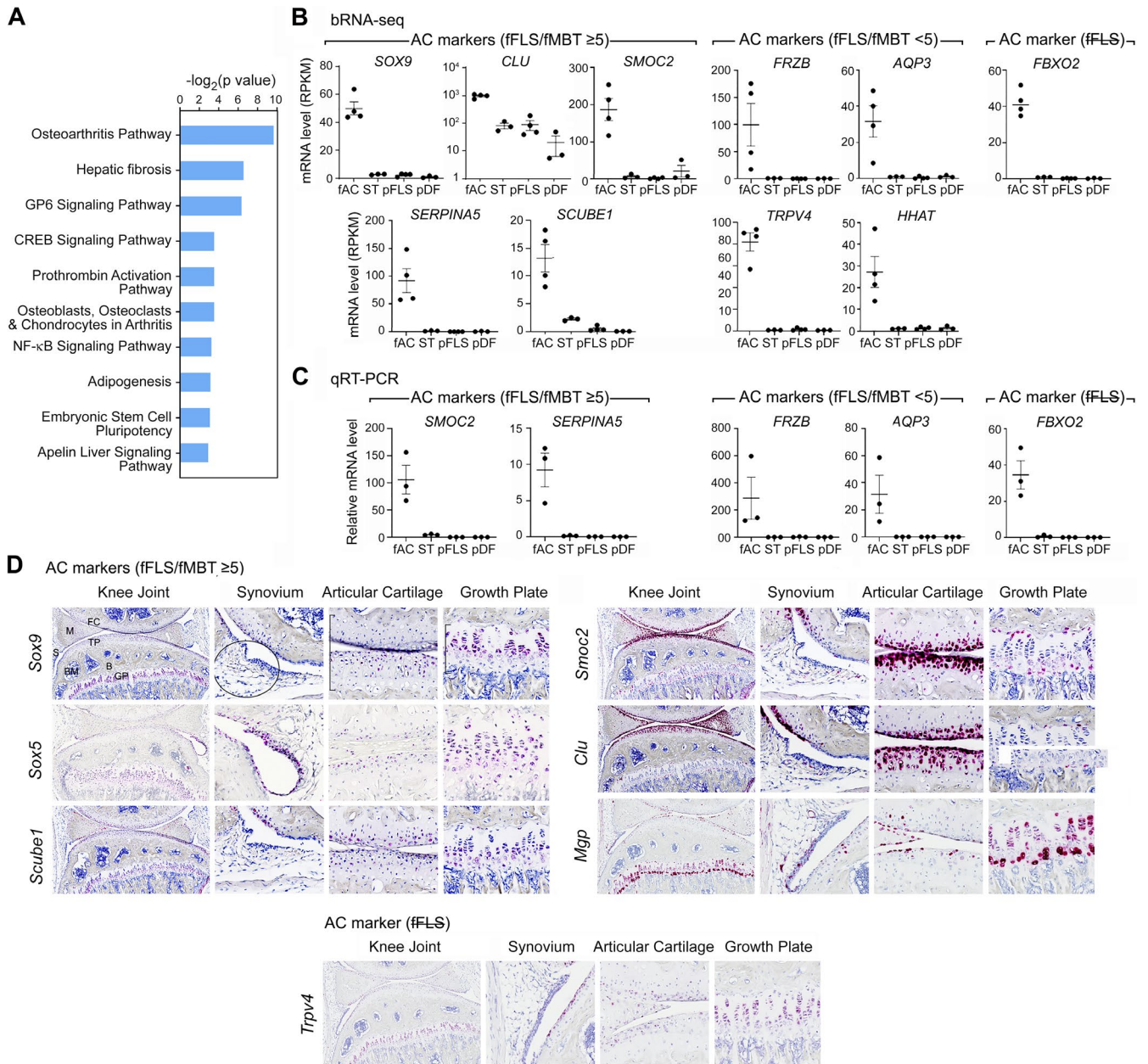


Figure 3. Validation of articular chondrocyte (AC) markers. **A**, Top 10 canonical pathways identified by an Ingenuity Pathway Analysis for the delineated list of AC markers (see Supplementary Table 6A). **B**, Messenger RNA (mRNA) levels of selected genes in each group of AC markers (see Supplementary Table 4D). Each dot represents a different freshly isolated articular chondrocyte (fAC), synovial tissue (ST), primary fibroblast-like synoviocyte (pFLS), or primary dermal fibroblast (pDF) sample. Means and SDs are indicated. **C**, Quantitative reverse transcription PCR (qRT-PCR) assay of selected AC markers. Three samples distinct from those used for bulk RNA sequencing (bRNA-seq) were used per sample type (see Supplementary Table 1). Data were normalized according to RNA levels for *TBP*. **D**, RNA in situ hybridization of adult mouse knee sections. For each gene, the left panel is a low-magnification picture showing femoral condyle (FC) and tibial plateau (TP) articular cartilage. Also seen are the meniscus (M), synovium tissue (S), tibia proximal growth plate (GP), bone (B), and bone marrow (BM). The other panels are high-magnification pictures of the synovium (circled), articular cartilage (bracket), and growth plate (bracket). RNA signals are detected with Fast Red. Cells are stained with hematoxylin (blue/purple). fFLS, freshly isolated fibroblast-like synoviocytes; fMBT, freshly isolated macrophages, T cells and B cells; RPKM, reads per kilobase per million mapped reads.

preferentially expressed in fAC (fAC/ST ratio ≥ 5), the second group comprised 5239 genes expressed at similar levels in fAC and ST (fAC/ST ratio < 5 but > 0.2), and the third group contained 906 genes exclusively or preferentially expressed in ST

(fAC/ST ratio ≤ 0.2). We next retained as AC candidate markers the 271 group 1 genes that were substantially expressed in fAC (RNA level ≥ 3 RPKM); as AC/FLS candidate markers, the 3810 group 2 genes substantially expressed in fAC and ST, and as

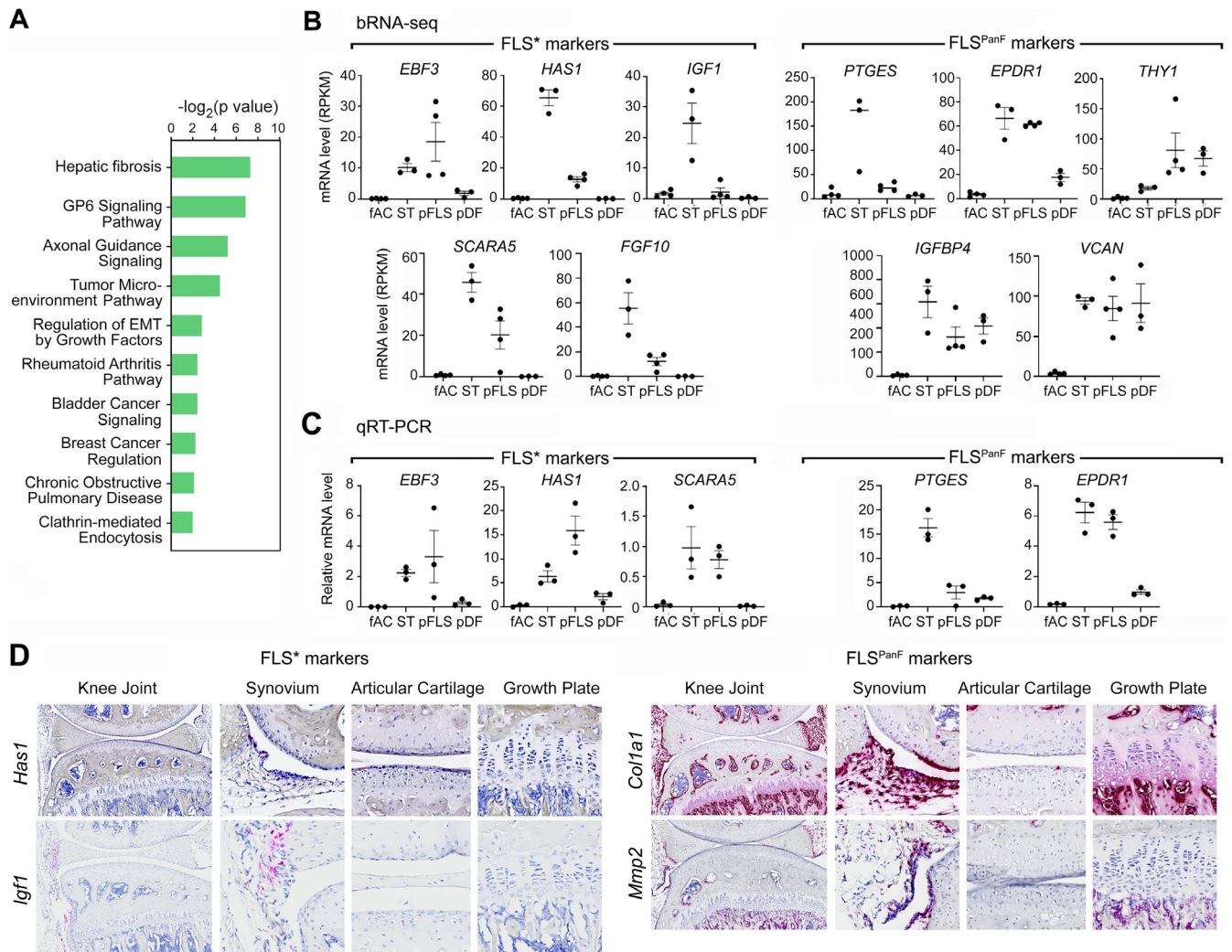


Figure 4. Validation of fibroblast-like synoviocyte (FLS) markers. **A**, Top 10 canonical pathways identified by Ingenuity Pathway Analysis of all joint-specific (*) and pan-fibroblastic (PanF) FLS (FLS* and FLS^{PanF}, respectively) markers combined (see Supplementary Table 6B). **B**, Messenger RNA (mRNA) levels of selected FLS* and FLS^{PanF} markers measured in bulk RNA sequencing (bRNA-seq) (see Supplementary Table 4F). **C**, Quantitative reverse transcription PCR (qRT-PCR) assay of selected FLS* and FLS^{PanF} markers performed with samples distinct from those used in bRNA-seq. Data are normalized with *TBP* RNA levels. **D**, RNA in situ hybridization of adult mouse knee sections for the indicated genes. The *Has1* and *Igf1* RNA signals were amplified to facilitate visualization. Data are presented as in Figure 3. EMT, epithelial-to-mesenchymal transition; fAC, freshly isolated articular chondrocyte; pDF, primary dermal fibroblast; pFLS, primary fibroblast-like synoviocyte; RPKM, reads per kilobase per million mapped reads; ST, synovial tissue.

FLS candidate markers, the 807 group 3 genes substantially expressed in ST.

Because ST contains multiple cell types, step three consisted of refining the candidate marker lists by using data from a recent study in which FLS, macrophages, T cells, and B cells were freshly isolated from the synovium of patients with RA and OA, sorted by flow cytometry, and analyzed in single-cell RNA-seq assays (7) (Supplementary Table 5A). UMAP of transcriptomes identified 17 subpopulations of cells (Supplementary Figure 1). Five corresponded to the previously described clusters of freshly isolated fibroblast-like synoviocytes (fFLS) F1 (cluster 4), F2 (cluster 1), F3 (cluster 11), and F4 (clusters 6 and 10). We globally refer to them as fFLS and to all other clusters as fMBT (freshly

isolated macrophages, B cells and T cells), except cluster 9, which is of a hybrid fFLS/fMBT phenotype. Of 11,962 genes significantly expressed in fFLS (RNA level ≥ 0.100 unique molecular identifier) (Supplementary Table 5A), 4545 were differentially expressed in our fAC, ST, pFLS, and pDF samples (Supplementary Table 5B). They included 156 AC, 3006 AC/FLS, and 544 FLS candidate markers (Figure 2A and Supplementary Table 4D–F).

In step four, we retained the 294 and 168 genes exclusively or preferentially expressed in fFLS, compared with fMBT (fFLS/fMBT ratio ≥ 5), as AC/FLS and FLS candidate markers, respectively. We did not apply this selection criterion to AC candidate markers because a lack of detection of 115 of them in fFLS supported genuine AC specificity. We thus kept all 271 AC candidate markers.

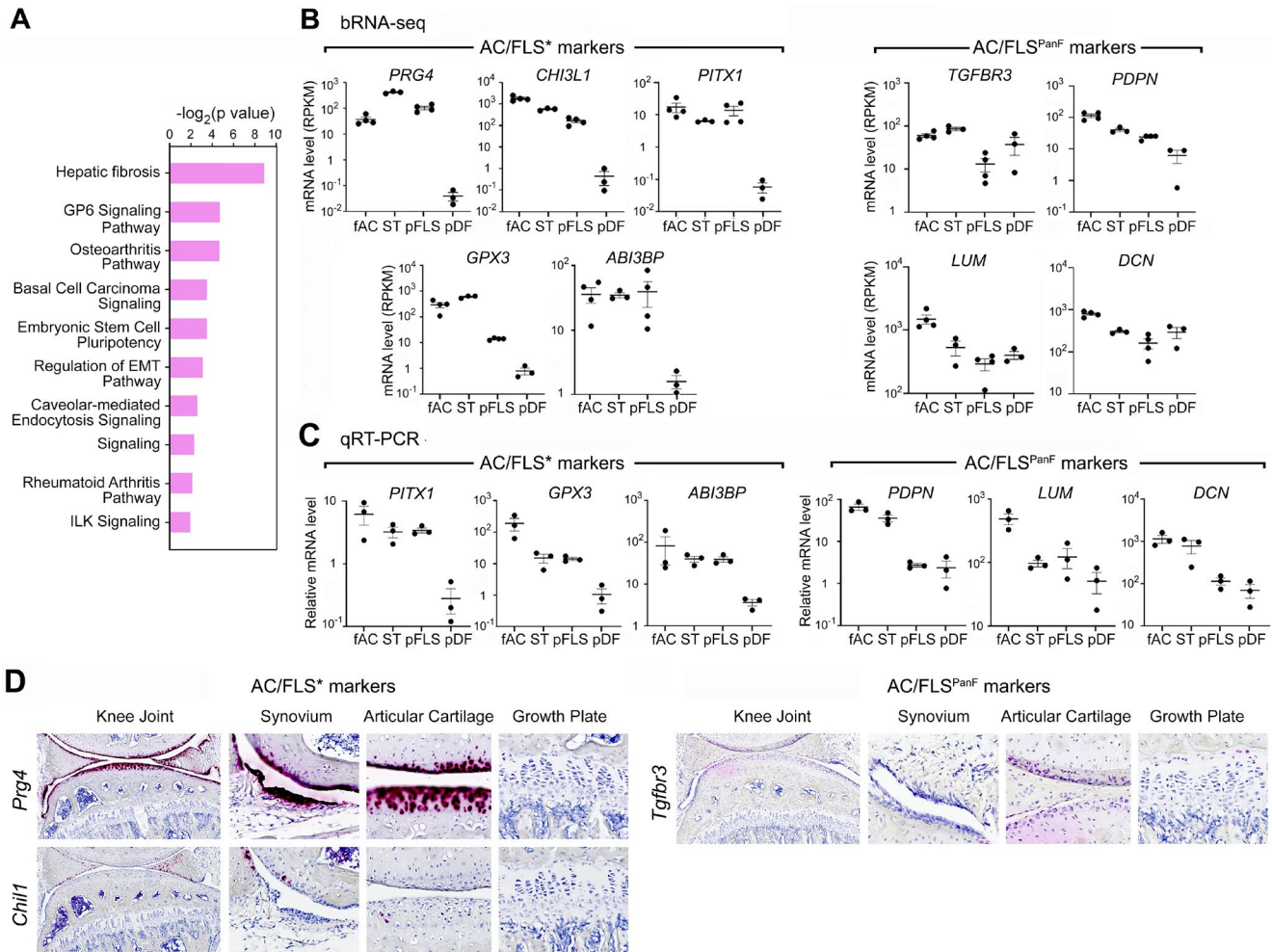


Figure 5. Validation of articular chondrocyte/fibroblast-like synoviocyte (AC/FLS) markers. **A**, Top 10 canonical pathways identified by Ingenuity Pathway Analysis of all joint-specific (*) and pan-fibroblastic (PanF) AC/FLS (AC/FLS* and AC/FLSPanF, respectively) markers combined (see Supplementary Table 6C). **B**, Messenger RNA (mRNA) levels of selected AC/FLS markers measured by bulk RNA sequencing (bRNA-seq) (see Supplementary Table 4E). **C**, Quantitative reverse transcription PCR (qRT-PCR) assay for selected AC/FLS markers performed using samples distinct from those used in bRNA-seq. Data were normalized with *TBP* RNA levels. **D**, RNA in situ hybridization of adult mouse knee sections for the indicated genes. Data are presented as in Figure 3. EMT, epithelial-to-mesenchymal transition; fAC, freshly isolated articular chondrocyte; ILK, integrin-linked kinase; pDF, primary dermal fibroblast; pFLS, primary fibroblast-like synoviocyte; RPKM, reads per kilobase per million mapped reads; ST, synovial tissue.

In step five, we retained 212 genes whose expression was unique or highly enriched in fAC, compared with pFLS and pDF (fAC/pFLS and fAC/pDF ratio ≥ 5), as presumptive AC markers. In parallel, we split the presumptive AC/FLS and FLS marker lists into two groups based on expression level in pFLS versus pDF, considering that genes similarly or weakly expressed in pFLS, compared with pDF (pFLS/pDF ratio < 5), were likely PanF, whereas others (pFLS/pDF ratio ≥ 5) were likely joint specific (*). We ended with 55 AC/FLS*, 239 AC/FLSPanF, 37 FLS*, and 131 FLSPanF presumptive markers.

Validating our delineation strategy, heat maps illustrated the enriched or exclusive expression of all types of markers in relevant fAC, ST, pFLS, and pDF samples (Figure 2B).

Together, these data consolidated the notion of a significant overlap of the AC and FLS transcriptome signatures and called for further marker validation and analysis.

Validation and analysis of the AC transcriptomic signature. Canonical pathway analyses validated our list of presumptive AC markers by identifying such joint-related pathways as OA, glycoprotein 6 (GP6), NF- κ B, and osteoblast/osteoclast/chondrocyte in arthritis among the 10 most significant pathways (9) (Figure 3A and Supplementary Table 6A).

The AC-specific expression of *SERPINA5*, *SMOC2*, *FRZB*, *FBXO2*, and *AQP3* was validated by qRT-PCR using samples independent of those used for bulk RNA-seq assays (Figure 3C).

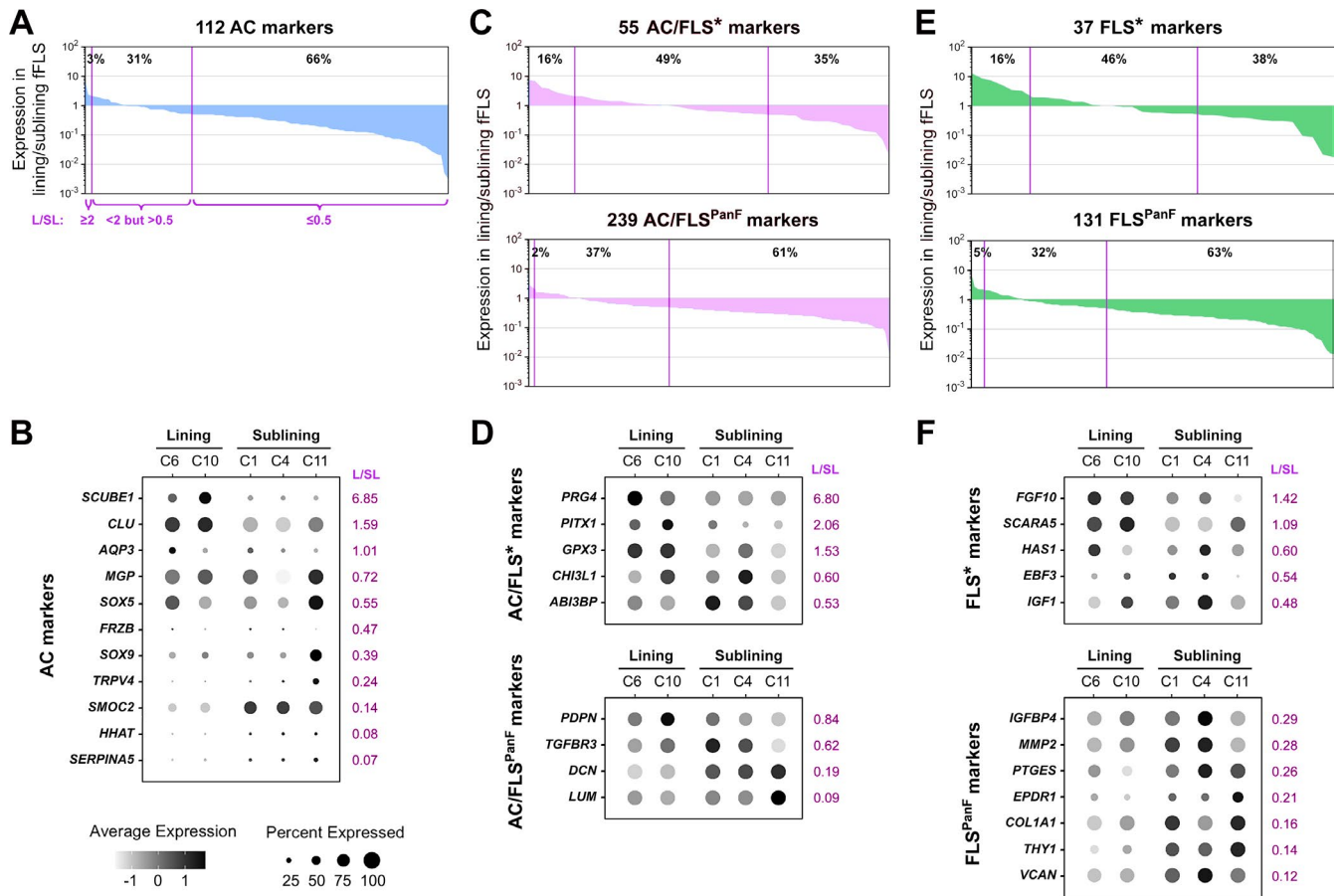


Figure 6. Differential expression of articular chondrocyte (AC), articular chondrocyte/fibroblast-like synoviocyte (AC/FLS), and fibroblast-like synoviocyte (FLS) marker genes across freshly isolated fibroblast-like synoviocyte (fFLS) subpopulations. **A**, **C**, and **E**, Graphs showing the relative expression of marker genes in lining (L) versus sublining (SL) fFLS (see Supplementary Table 4D–F). Genes were ranked on the x-axis in descending order of their L/SL expression ratios. Vertical lines separate the genes in three groups according to this ratio, as indicated. The percentages of markers present in each group are indicated. **B**, **D**, and **F**, Dot plots showing the relative expression levels of selected marker genes across all fFLS clusters. The size and darkness of the dots reflect the proportions of expressing cells and the average RNA levels in these cells, respectively. L/SL ratios are indicated. *Joint specific. PanF, pan-fibroblastic.

Moreover, RNA in situ hybridization of adult mouse knees showed *Sox9* and *Sox5* expression in AC and GPC, as expected (Figure 3D). Interestingly, it detected significant expression of *Sox5*, but not *Sox9*, in ST-lining cells. This finding was consistent with the fAC/ST ratios of 5.93 and 17.75 determined, respectively, for *SOX5* and *SOX9*. *Scube1* expression was readily detected in intermediate-zone AC and GPC, but not in ST. *Smoc2*, *Clu*, *Mgp*, and *Trpv4* were expressed highly in nonmineralizing AC, modestly in mineralizing AC and in GPC, and very weakly in ST stroma (Figure 3D). These data thus further validated these genes as genuine AC markers.

Validation and analysis of the FLS transcriptomic signature. Canonical pathway analyses validated our presumptive FLS marker list by linking it to GP6 signaling and RA (Figure 4A and Supplementary Table 6B). Other pathways in the top 10 were related to cancer and epithelial-to-mesenchymal transition (EMT), likely reflecting well-known proliferative and migratory properties of FLS.

Many presumptive FLS* markers were not previously recognized as such. They included early B-cell factor 3 (*EBF3*), hyaluronan synthase 1 (*HAS1*), insulin growth factor 1 (*IGF1*), scavenger receptor class A member 5 (*SCARA5*), and fibroblast growth factor 10 (*FGF10*) (Figure 4B and Supplementary Table 4F). Many well-established PanF markers were found on the list of FLS^{PanF} markers, including *THY1* (cell surface antigen CD90), insulin-like growth factor binding protein 4 (*IGFBP4*), *VCAN*, fibulin 2 (*FBLN2*) (an extracellular matrix glycoprotein), and *COL1A1* (Figure 4B and Supplementary Table 4F). Numerous genes were also newly identified as FLS^{PanF} markers, including prostaglandin E synthase (*PTGES*), ependymin related 1 (*EPDR1*), and matrix metalloproteinase 2 (*MMP2*). The specificity of new markers was confirmed by qRT-PCR (Figure 4C). In addition, RNA in situ hybridization of mouse knees validated the FLS* identity of *Has1* and *Igf1* and the FLS^{PanF} identity of *Col1a1* and *Mmp2* (Figure 4D).

Together, these data indicated that FLS distinguish themselves from AC by the expression of both highly specific genes and PanF genes that do or may contribute essential functions.

Validation and analysis of the AC/FLS transcriptomic signature. Having validated the AC and FLS signatures, we next proceeded with the presumptive AC/FLS signature. Interestingly, even though the AC, FLS, and AC/FLS signatures were composed of different genes, canonical pathway analyses showed several overlaps. Namely, the AC/FLS signature shared GP6 signaling with the AC and FLS signatures; OA, with the AC signature; and RA and EMT regulation, with the FLS signature (Figure 5A and Supplementary Table 6C). This suggested that a significant number of AC/FLS markers complement AC and FLS markers to fulfill joint-specific functions. This said, the high ranking of such pathways as HIPPO signaling and integrin-linked kinase signaling, for the AC/FLS signature only, suggested that many AC/FLS markers may assume specific functions, including the control of cell-cell and cell-matrix interactions.

AC/FLS* markers included *PRG4*, as expected (Figure 5B and Supplementary Table 4E), and previously uncharacterized joint markers, such as chitinase-3-like-1 protein (*CHI3L1*), paired-like homeodomain 1 (*PITX1*), glutathione peroxidase 3 (*GPX3*), and ABI family member 3 binding protein (*ABI3BP*). AC/FLS^{PanF} markers included transforming growth factor- β receptor 3 (*TGFBR3*) and well-known PanF markers, such as podoplanin (*PDPN*), lumican (*LUM*), and decorin (*DCN*) (Figure 5B).

qRT-PCR assays validated that *PITX1*, *GPX3*, and *ABI3BP* were more strongly expressed in fAC, ST, and pFLS than in pDF (Figure 5C) and that *PDPN*, *LUM*, and *DCN* were highly expressed in fAC and ST and similarly expressed in pFLS and pDF (Figure 5E). RNA in situ hybridization of mouse knees confirmed the exclusive expression of *Prg4* in ST-lining cells and non-mineralizing AC (Figure 5D). *Chil1* (orthologue of *CHI3L1*) was expressed in intermediate-zone AC, but not in ST, possibly revealing differential expression of the human and mouse orthologues, and *Tgfb3* was moderately expressed in AC and ST-lining cells (Figure 5D).

These analyses thus validated the existence of a significant AC/FLS transcriptome signature, whose critical function is already established for several genes and warrants investigation for others.

Differential expression patterns of AC, FLS, and AC/FLS markers in AC and ST. In situ data suggested that AC, FLS, and AC/FLS markers vary in spatial distribution within AC and ST. To consolidate this finding and determine whether the AC/FLS signature characterizes discrete AC and FLS subpopulations, we analyzed the distribution of all genes constituting our marker lists in the five fFLS subpopulations identified by single-cell RNA-seq assays. For this, we calculated the expression level of each gene in joint-space lining fFLS (clusters 6 and 10) relative to that in sublining (stromal) fFLS (clusters 1, 4, and 11)

(Supplementary Table 4D–F). Profiles obtained by plotting these ratios in descending order revealed that two-thirds (66%) of the AC markers detected in fFLS were most strongly expressed in sublining fFLS (Figure 6A). These genes included *SOX9*, *TRPV4*, *SMOC2*, *HHAT*, and *SERPINA5* (Figure 6B). Most others (31%), including *CLU*, *AQP3*, *MGP*, and *SOX5*, were similarly expressed in lining and sublining fFLS, whereas the remaining ones (3%), including *SCUBE1*, were preferentially expressed in sublining fFLS. Notably, many AC markers, namely *AQP3*, *FRZB*, *TRPV4*, *HHAT*, and *SERPINA5*, were expressed by very few cells (less than 25%) in each fFLS cluster, a finding consistent with strong AC enrichment. Other genes were primarily expressed in one fFLS cluster, such as C10 lining fFLS for *SCUBE1* and C11 sublining fFLS for *SOX9*. The remaining markers, namely *CLU*, *MGP*, and *SOX5*, were expressed by most cells in both lining and sublining fFLS clusters. These differences emphasize the notion that cell-type specificity is a relative notion and that sums of varying, rather than uniform, marker gene expression patterns render cell type-specific transcriptomic signatures.

Interestingly, AC/FLS^{PanF} and FLS^{PanF} markers closely resembled AC markers in their differential expression patterns in lining versus sublining fFLS (Figure 6C–F). This finding, together with the fact that most selected markers were expressed in almost all cells within fFLS clusters, strongly suggested that AC, AC/FLS^{PanF}, and FLS^{PanF} markers are co-expressed by FLS, and possibly also by AC, rather than expressed by distinct subpopulations of cells.

Unlike AC, AC/FLS^{PanF}, and FLS^{PanF} markers, almost half of the AC/FLS* and FLS* markers (49% and 46%, respectively) were evenly expressed in lining and sublining fFLS, and about one-third (35% and 38%, respectively) were mostly expressed in sublining fFLS. The remaining 16% were predominantly expressed in lining cells and likely reflected unique properties of joint-space lining fFLS and AC.

Taken together, these results indicated that the AC/FLS transcriptomic features do not belong to discrete AC and FLS subpopulations but are distributed in a differential manner among all cell subpopulations.

DISCUSSION

This study deepened knowledge of the transcriptomic features of human adult AC and synovial fibroblasts. By newly identifying dozens of unique AC and FLS markers, it expanded the concept that the two cell types distinguish themselves by the expression of specific gene sets. Interestingly, it unexpectedly exposed that AC and FLS also express common (AC/FLS) markers and that these markers outnumber the unique markers. Additionally, AC, FLS, and AC/FLS markers were found to overlap in their expression patterns and, altogether, span all AC and FLS subpopulations. These findings thus strongly suggest that AC and FLS are governed by a mosaic of shared and distinct cell

type-specific regulatory mechanisms; together with new high-throughput data resources, they should help increase understanding and improve treatments of joint diseases.

The distinctive compositions and properties of the articular cartilage and synovium explain that AC and FLS differ for a series of markers that include well-known extracellular matrix components. Many of the AC and FLS markers newly identified in this study can be predicted to participate in essential cell fate determination, differentiation, and functions. These markers likely reflect the healthy status of the tissues because we only used samples procured from young adult to middle-aged donors and carefully selected them on the basis of health history and tissue appearance. Additionally, the transcriptome signatures were shared by all donors and validated in healthy mice. We cannot fully exclude, however, that some markers of the young healthy condition were missed because of possible downregulation in early adulthood, and, vice versa, that genes may be present on our marker lists because they are upregulated in early aging or in early joint disease.

Genes identified here as genuine FLS markers (FLS*) include *HAS1*, which encodes an enzyme synthesizing hyaluronan, a major synovial fluid component and whose deficiency causes chronic joint inflammation in mice (16). Genes identified here as genuine AC markers include the gene for the chaperone clusterin (apolipoprotein J), an OA biomarker with antiinflammatory properties (17–19). They also include *HHAT* and *SCUBE1*, which likely modulate hedgehog signaling. The hedgehog pathway is pivotal in skeletogenesis, including joint morphogenesis. Its importance in adult articular cartilage homeostasis has been suggested (20), and the deleterious consequence of its overt activation is well documented in OA (21). *HHAT* catalyzes the attachment of palmitate onto hedgehog, an event required for long-range signaling (22), and *Hhat* knockout mice exhibit skeletal dysplasia (14). *HHAT* may thus critically modulate hedgehog signaling in AC. *SCUBE* proteins are secreted and membrane-tethered factors controlling the secretion of cholesterol-modified hedgehog ligands (23). *SCUBE2* encodes a potent regulator of Indian hedgehog during endochondral ossification (24). *SCUBE1*, which is downregulated in OA cartilage, may thus be pivotal in joint homeostasis. FGF signaling is essential in various aspects of skeleton development and disease (25), including articular cartilage homeostasis and OA (26). Accordingly, genuine AC markers include *FGFR2* and *FGFR3*, as well as *FGFBP2*, which encodes an FGF-binding protein that mobilizes FGFs from extracellular matrices (27). No specific FGF gene was found expressed in AC, but *FGF10* was identified as an FLS* marker. It is required for limb formation (28), but its role in adult joints remains unknown. Furthermore, our data suggest determining roles for secreted frizzled-related proteins (SFRPs) in joints. These Wingless and Int-1 (WNT) pathway inhibitors play important roles in cartilage development, homeostasis, and pathology (29). Downregulation of *FRZB*, which encodes SFRP3, has been linked to OA progression, and SFRP3 may prevent AC

degradation (30,31) and have an antiinflammatory effect on FLS (32). Thus, an interplay between AC-produced SFRP3 and FLS-produced SFRP4 may ensure joint homeostasis.

Evidence that AC and FLS share markers was previously provided. A well-known example is *PRG4*, which encodes a proteoglycan participating in joint lubrication. Surprising was the large number of markers shared by the two cell types. Some of these markers encode other extracellular matrix components, such as *CHI3L1*. Its role in joint homeostasis remains unclear, but it has been shown to be an RA and OA biomarker and to be implicated in tissue remodeling (33). AC/FLS markers also include genes needed for FLS and AC survival and unique joint functions. The signaling pathways best represented by AC/FLS markers were indeed the glucocorticoid receptor and circadian rhythm pathways, which have important joint homeostasis functions (34–36). These findings should motivate future studies to assess the importance of new distinct and shared markers of AC and FLS.

The uncovering of a large overlap of the AC and FLS signatures raised a key question on whether AC/FLS markers reflect the existence of a cell type or subtype common to both the articular cartilage and synovium. Lining FLS and superficial AC were obvious candidates because both are in direct contact with the synovial cavity and highly express *PRG4*. Single-cell RNA-seq and RNA in situ hybridization assays, however, convincingly showed that the genes composing the AC/FLS signature exhibit differential expression patterns and are expressed in both lining and sublining regions of the tissues. Furthermore, the percentages of cells expressing AC/FLS, AC, and FLS markers in these regions were found to be high enough to conclude that many cells express AC/FLS markers, in addition to AC or FLS markers, and thus that the two tissues house multiple phenotypically overlapping cell populations.

The large overlap of the AC and FLS signatures also raises a question on the genetic mechanisms that control the phenotypes of these cells. One possibility is that joints are governed by a mosaic of regulatory menus, including pan-cartilaginous, AC-specific, PanF, FLS-specific, and AC/FLS programs. *SOX9* is well known to activate the pan-cartilaginous program, and although it is unclear whether it participates in the AC program, it is unlikely to be involved in the AC/FLS program because it is hardly expressed in FLS. The factors driving the FLS, AC, and AC/FLS programs remain unknown. Their identification in future research will be crucial to understanding key nodes in joint-specific developmental, physiological, and pathogenetic mechanisms and thereby designing tailored strategies to effectively prevent joint degeneration and repair or regenerate healthy joints. Newly discovered joint markers will be helpful in such efforts, namely as exquisite tools to probe molecular mechanisms and genetically target discrete cell populations.

In conclusion, by extending knowledge of the molecular signatures of human AC and FLS and revealing a large overlap between these signatures, this study brings into light that AC and

FLS populations represent a series of variants of a unique joint-specific cell type rather than distinct cell types. This new concept will have to be taken into full consideration when further dissecting mechanisms underlying joint physiology and pathology and when seeking to improve preventive, therapeutic, and regenerative strategies for joint diseases.

ACKNOWLEDGMENTS

Drs. Lefebvre and Bhattaram thank support from their former institution, the Cleveland Clinic Lerner Research Institute, where they initiated this study. They also thank G. F. Muschler, S. A. Lietman, and N. W. Mesko for providing cartilage and synovium tissue samples, A. Kowalczyk for providing dermal fibroblasts, and A. Arif and S. Ramirez-Perez for advice during manuscript preparation.

AUTHOR CONTRIBUTIONS

All authors were involved in drafting the article and revising it for intellectual content, and all authors approved the final version to be published. Drs. Lefebvre and Bhattaram had full access to all of the data in the study and take responsibility for the integrity of the data and the accuracy of the data analysis.

Study conception and design. Lefebvre, Bhattaram.

Acquisition of data. Jones, Angelozzi, Gangishetti, Haseeb, de Charleroy, Lefebvre, Bhattaram.

Analysis and interpretation of data. Jones, Angelozzi, Lefebvre, Bhattaram.

REFERENCES

- Decker RS. Articular cartilage and joint development from embryogenesis to adulthood. *Semin Cell Dev Biol* 2017;62:50–6.
- Bhattaram P, Chandrasekharan U. The joint synovium: a critical determinant of articular cartilage fate in inflammatory joint diseases. *Semin Cell Dev Biol* 2017;62:86–93.
- Rux D, Decker RS, Koyama E, Pacifici M. Joints in the appendicular skeleton: developmental mechanisms and evolutionary influences. *Curr Top Dev Biol* 2019;133:119–51.
- Liu C-F, Angelozzi M, Haseeb A, Lefebvre V. SOX9 is dispensable for the initiation of epigenetic remodeling and the activation of marker genes at the onset of chondrogenesis. *Development* 2018;145:dev164459.
- Napierala JS, Li Y, Lu Y, Lin K, Hauser LA, Lynch DR, et al. Comprehensive analysis of gene expression patterns in Friedreich's ataxia fibroblasts by RNA sequencing reveals altered levels of protein synthesis factors and solute carriers. *Dis Model Mech* 2017;10:1353–69.
- Zhang F, Wei K, Slowikowski K, Fonseka CY, Rao DA, Kelly S, et al. Defining inflammatory cell states in rheumatoid arthritis joint synovial tissues by integrating single-cell transcriptomics and mass cytometry. *Nat Immunol* 2019;20:928–42.
- Hafemeister C, Satija R. Normalization and variance stabilization of single-cell RNA-seq data using regularized negative binomial regression. *Genome Biol* 2019;20:296.
- Bhattaram P, Muschler G, Wixler V, Lefebvre V. Inflammatory cytokines stabilize SOXC transcription factors to mediate the transformation of fibroblast-like synoviocytes in arthritic disease. *Arthritis Rheumatol* 2018;70:371–82.
- Nurden AT. Clinical significance of altered collagen-receptor functioning in platelets with emphasis on glycoprotein VI. *Blood Rev* 2019;38:100592.
- James IE, Kumar S, Barnes MR, Gress CJ, Hand AT, Dodds RA, et al. FrzB-2: a human secreted frizzled-related protein with a potential role in chondrocyte apoptosis. *Osteoarthritis Cartilage* 2000;8:452–63.
- Hagiwara K, Shinozaki T, Matsuzaki T, Takata K, Takagishi K. Immunolocalization of water channel aquaporins in human knee articular cartilage with intact and early degenerative regions. *Med Mol Morphol* 2013;46:104–8.
- Marchant TW, Johnson EJ, McTeir L, Johnson CI, Gow A, Liuti T, et al. Canine brachycephaly is associated with a retrotransposon-mediated missplicing of SMOC2. *Curr Biol* 2017;27:1573–84.
- Boeuf S, Steck E, Peltari K, Hennig T, Buneb A, Benz K, et al. Subtractive gene expression profiling of articular cartilage and mesenchymal stem cells: serpins as cartilage-relevant differentiation markers. *Osteoarthritis Cartilage* 2008;16:48–60.
- Dennis JF, Kurosaka H, Iulianella A, Pace J, Thomas N, Beckham S, et al. Mutations in hedgehog acyltransferase (Hhat) perturb hedgehog signaling, resulting in severe acrania-holoprosencephaly-agnathia craniofacial defects. *PLoS Genet* 2012;8:e1002927.
- Atkin G, Hunt J, Minakawa E, Sharkey L, Tipper N, Tennant W, et al. F-box only protein 2 (Fbxo2) regulates amyloid precursor protein levels and processing. *J Biol Chem* 2014;289:7038–48.
- Chan DD, Xiao WF, Li J, de la Motte CA, Sandy JD, Plaas A. Deficiency of hyaluronan synthase 1 (Has1) results in chronic joint inflammation and widespread intra-articular fibrosis in a murine model of knee joint cartilage damage. *Osteoarthritis Cartilage* 2015;23:1879–89.
- Kozhemyakina E, Zhang M, Ionescu A, Ayturk UM, Ono N, Kobayashi A, et al. Identification of a Prg4-expressing articular cartilage progenitor cell population in mice. *Arthritis Rheumatol* 2015;67:1261–73.
- Duffy T, Bekki H, Lotz MK. Genome-wide occupancy profiling reveals critical roles of FOXO1 in regulating extracellular matrix and circadian rhythm genes in human chondrocytes. *Arthritis Rheumatol* 2020;72:1514–23.
- Fernandez-Puente P, Gonzalez-Rodriguez L, Calamia V, Picchi F, Lourido L, et al. Analysis of endogenous peptides released from osteoarthritic cartilage unravels novel pathogenic markers. *Mol Cell Proteomics* 2019;18:2018–28.
- Chen X, Macica CM, Nasiri A, Broadus AE. Regulation of articular chondrocyte proliferation and differentiation by Indian hedgehog and parathyroid hormone-related protein in mice. *Arthritis Rheum* 2008;58:3788–97.
- Lin AC, Seeto BL, Bartoszko JM, Khoury MA, Whetstone H, Ho L, et al. Modulating hedgehog signaling can attenuate the severity of osteoarthritis. *Nat Med* 2009;15:1421–5.
- Koleva MV, Rothery S, Spitaler M, Neil MA, Magee AI. Sonic hedgehog multimerization: a self-organizing event driven by post-translational modifications? *Mol Membr Biol* 2015;32:65–74.
- Creanga A, Glenn TD, Mann RK, Saunders AM, Talbot WS, Beachy PA. Scube/You activity mediates release of dually lipid-modified hedgehog signal in soluble form. *Genes Dev* 2012;26:1312–25.
- Lin YC, Roffler SR, Yan Y-T, Yang R-B. Disruption of scube2 impairs endochondral bone formation. *J Bone Miner Res* 2015;30:1255–67.
- Ornitz DM, Marie PJ. Fibroblast growth factors in skeletal development. *Curr Top Dev Biol* 2019;133:195–234.
- Valverde-Franco G, Binette JS, Li W, Wang H, Chai S, Laflamme F, et al. Defects in articular cartilage metabolism and early arthritis in fibroblast growth factor receptor 3 deficient mice. *Hum Mol Genet* 2006;15:1783–92.
- Taetzsch T, Brayman VL, Valdez G. FGF binding proteins (FGFBPs): modulators of FGF signaling in the developing, adult, and stressed nervous system. *Biochim Biophys Acta Mol Basis Dis* 2018;1864(Pt B):2983–91.
- Jin L, Wu J, Bellusci S, Zhang J-S. Fibroblast growth factor 10 and vertebrate limb development. *Front Genet* 2019;9:705.

29. Claudel M, Jouzeau J-Y, Cailotto F. Secreted frizzled-related proteins (sFRPs) in osteo-articular diseases: much more than simple antagonists of Wnt signaling? *FEBS J* 2019;286:4832–51.
30. Thysen S, Luyten FP, Lories RJ. Loss of Frzb and Sfrp1 differentially affects joint homeostasis in instability-induced osteoarthritis. *Osteoarthritis Cartilage* 2015;23:275–9.
31. Killock D. Osteoarthritis: Frzb knockout reveals the complexity of Wnt signaling in joint homeostasis. *Nat Rev Rheumatol* 2012;8:123.
32. Elhaj Mahmoud D, Sassi N, Drissi G, Barsaoui M, Zitouna K, Sahli H, et al. sFRP3 and DKK1 regulate fibroblast-like synoviocytes markers and Wnt elements expression depending on cellular context. *Immunol Invest* 2017;46:314–28.
33. Vaananen T, Lehtimaki L, Vuolteenaho K, Hamalainen M, Oksa P, Vierikko T, et al. Glycoprotein YKL-40 levels in plasma are associated with fibrotic changes on HRCT in asbestos-exposed subjects. *Mediators Inflamm* 2017;2017:1797512.
34. Tu J, Stoner S, Fromm PD, Wang T, Chen D, Tuckermann J, et al. Endogenous glucocorticoid signaling in chondrocytes attenuates joint inflammation and damage. *FASEB J* 2018;32:478–87.
35. Dudek M, Gossan N, Yang N, Im H-J, Ruckshanthi JP, Yoshitane H, et al. The chondrocyte clock gene Bmal1 controls cartilage homeostasis and integrity. *J Clin Invest* 2016;126:365–76.
36. Hand LE, Dickson SH, Freemont AJ, Ray DW, Gibbs JE. The circadian regulator Bmal1 in joint mesenchymal cells regulates both joint development and inflammatory arthritis. *Arthritis Res Ther* 2019;21:5.